Supporting Information –

Cobalt Nanoparticles Embedded in Nitrogen-Doped Carbon for the Hydrogen Evolution Reaction

*Huilong Fei,[†] Yang Yang,[†,‡] Zhiwei Peng,[†] Gedeng Ruan,[†] Qifeng Zhong,[†] Lei Li,[†] Errol L. G. Samuel,[†] and James M. Tour[†,‡,§,]**

[†]Department of Chemistry, [‡] Smalley Institute for Nanoscale Science and Technology,[§]Department of Materials Science and NanoEngineering, Rice University, 6100 Main Street, Houston, Texas 77005, USA

**E-mail: tour@rice.edu*

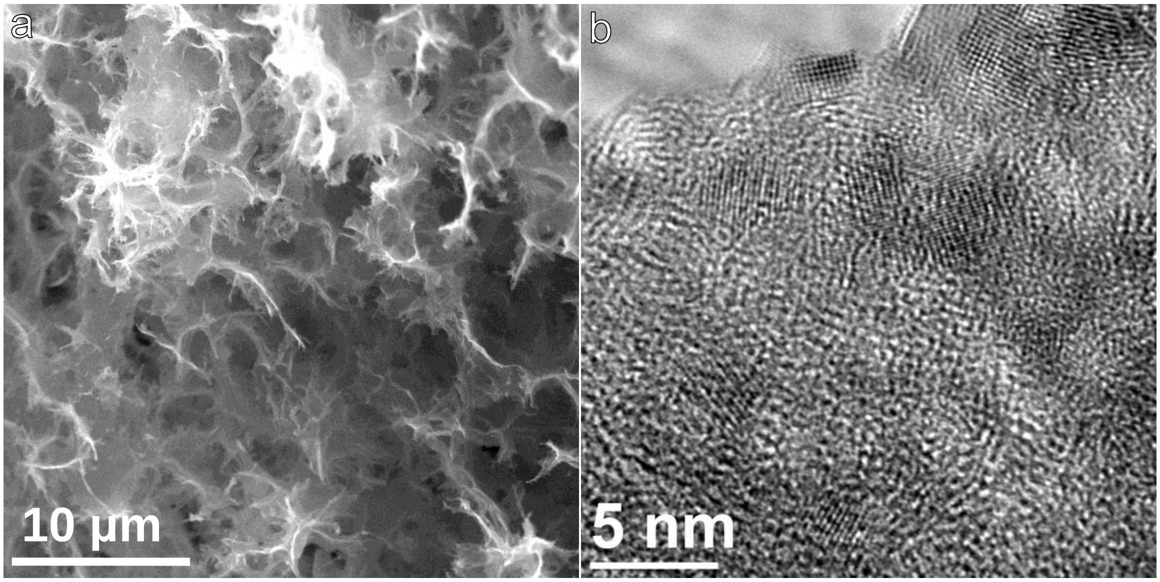

Figure S1. Morphology characterizations of CoO-G. (a) SEM image of CoO-G prepared by a hydrothermal reaction. (b) TEM image of CoO-G.

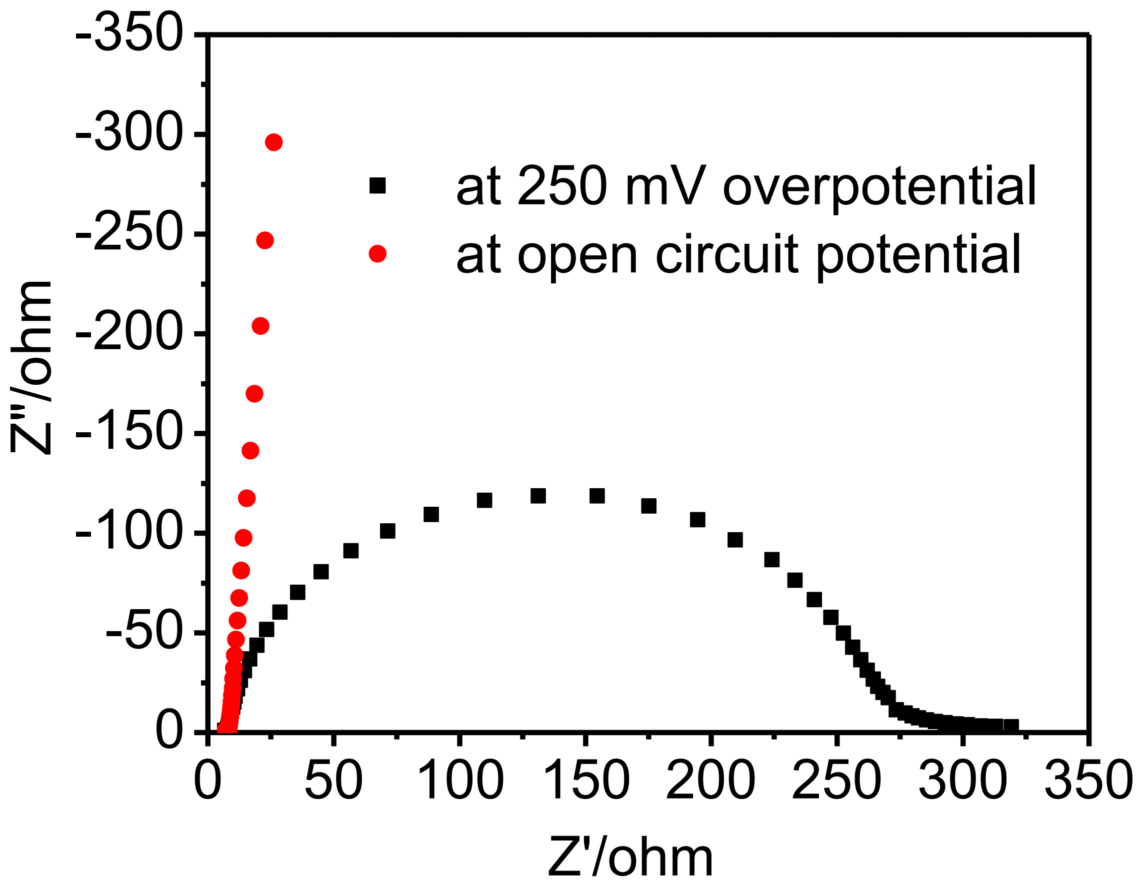

Figure S2. Electrochemical impedance spectra of N-Co@G performed at open circuit potential and η = 200 mV *vs* RHE from 100 kHz to 0.1 Hz.

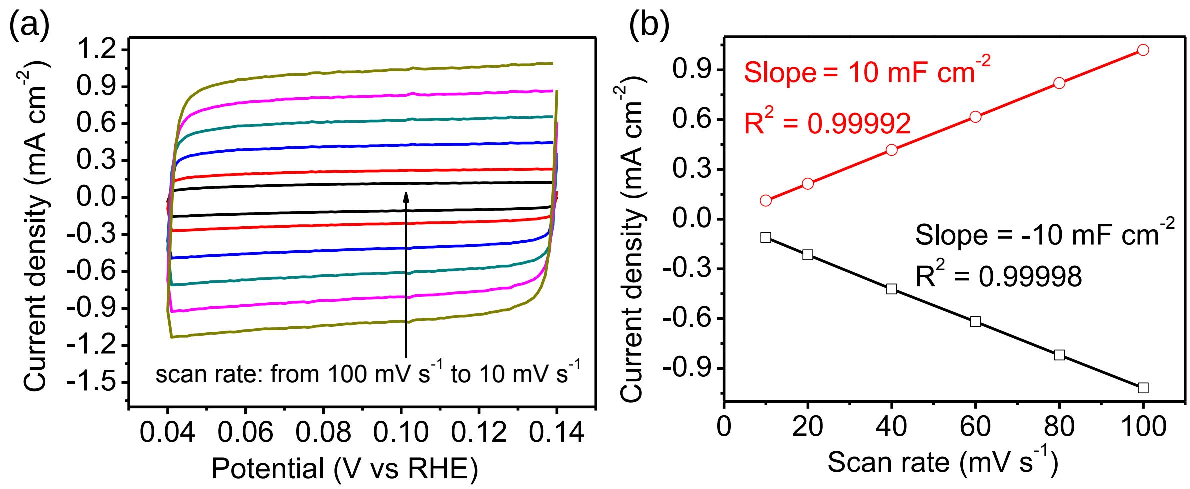

Figure S3. (a) CVs measured in a non-Faradaic region (± 50 mV *vs* open circuit potential) at different scan rates from 100 to 10 mV s^{-1}. (b) The cathodic (black) and anodic (red) charging current measured at 0.09 V vs RHE plotted as a function of scan rate. The double layer capacitance is taken as the average of the absolute value of the slope of the linear fits to the data.

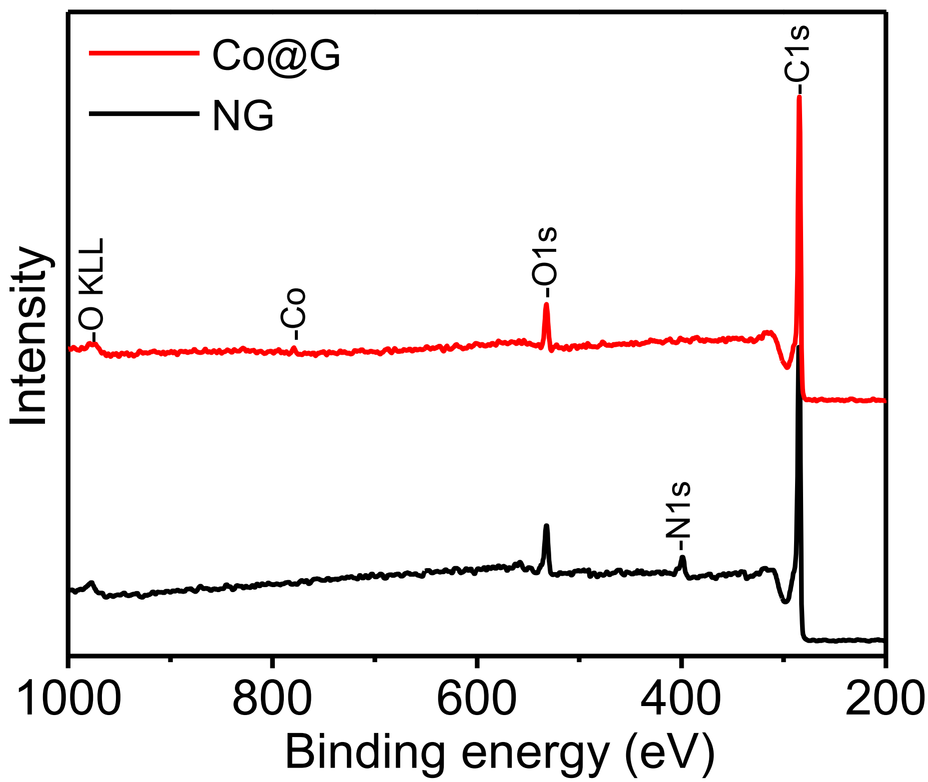

Figure S4. XPS survey spectra of the control samples of Co@G and NG.

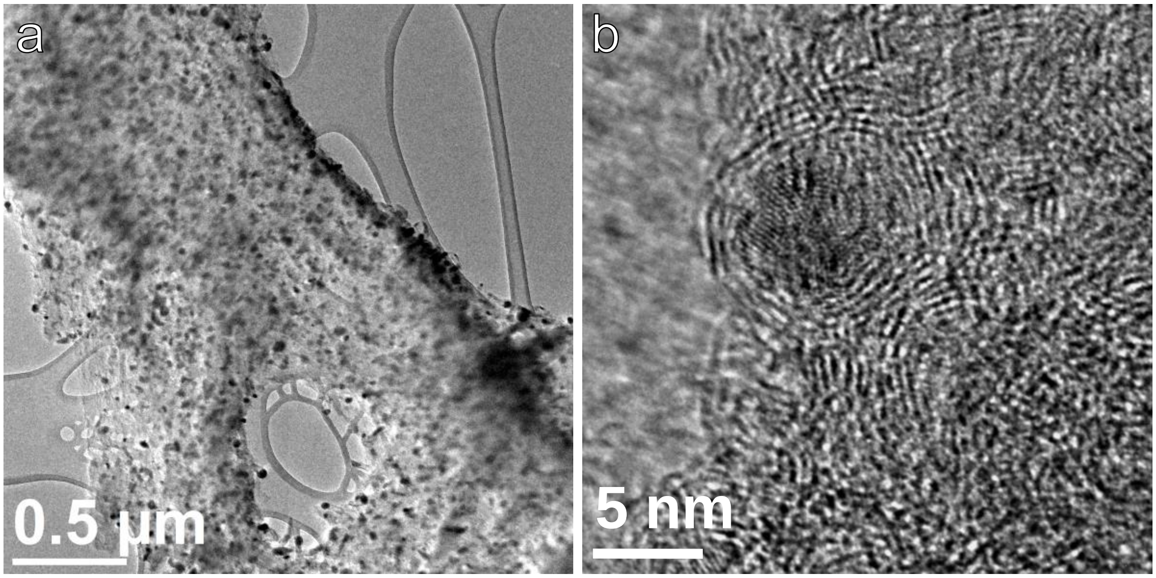

Figure S5. TEM image of N-Fe@G at (a) low and (b) high magnifications. N-Fe@G has similar morphologic characteristics to N-Co@G, with small nanoparticles decorating on the graphene sheets and each individual nanoparticle has core-shell structure with Fe encapsulated in carbon layers.

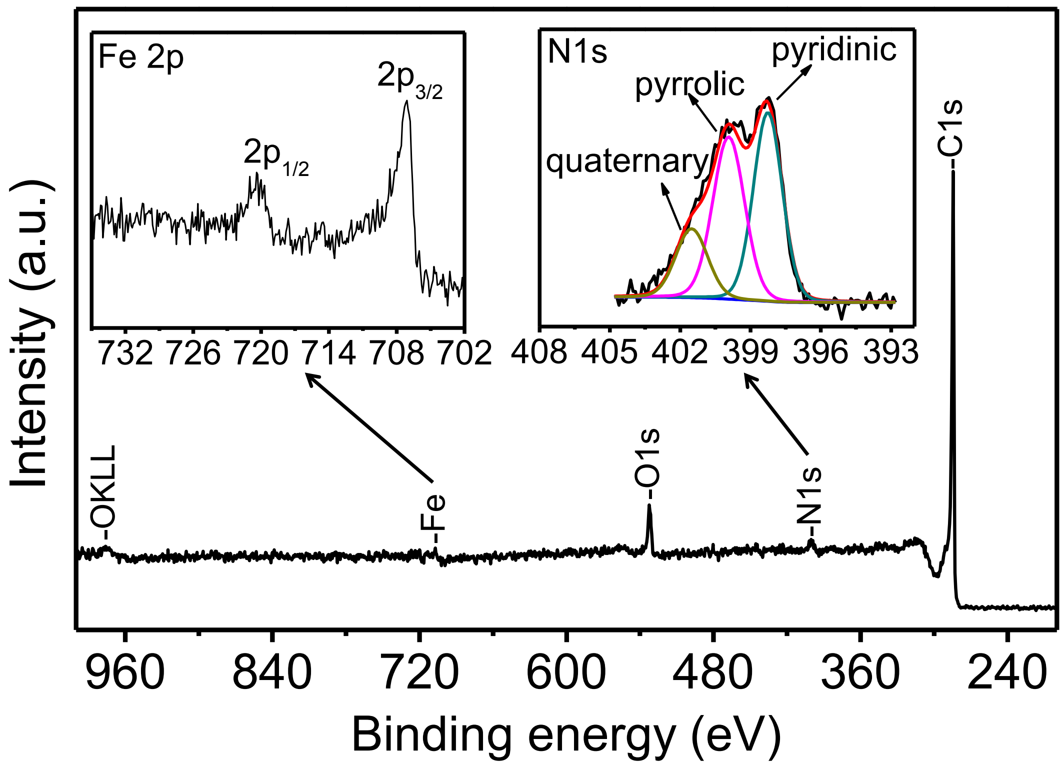

Figure S6. XPS spectra of N-Fe@G, showing the presence of C, O, N and Fe elements. The Fe is in metallic form and the N has three different species of pyridinic, pyrrolic and quaternary configurations.

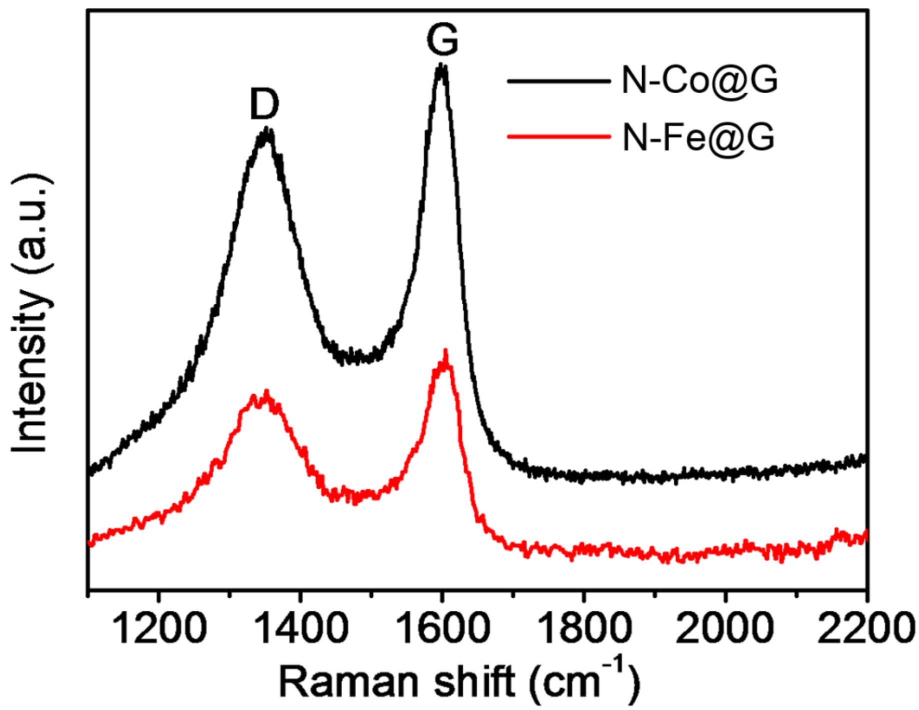

Figure S7. Raman spectra of N-Co@G and N-Fe@G. The spectra show the characteristic D and G bands for carbon, which are associated with the disordered carbon and sp^2-hybridized graphitic carbon, respectively. The similar intensity ratio of D to G band in these two samples indicates the similar degree of the carbon crystallinity.

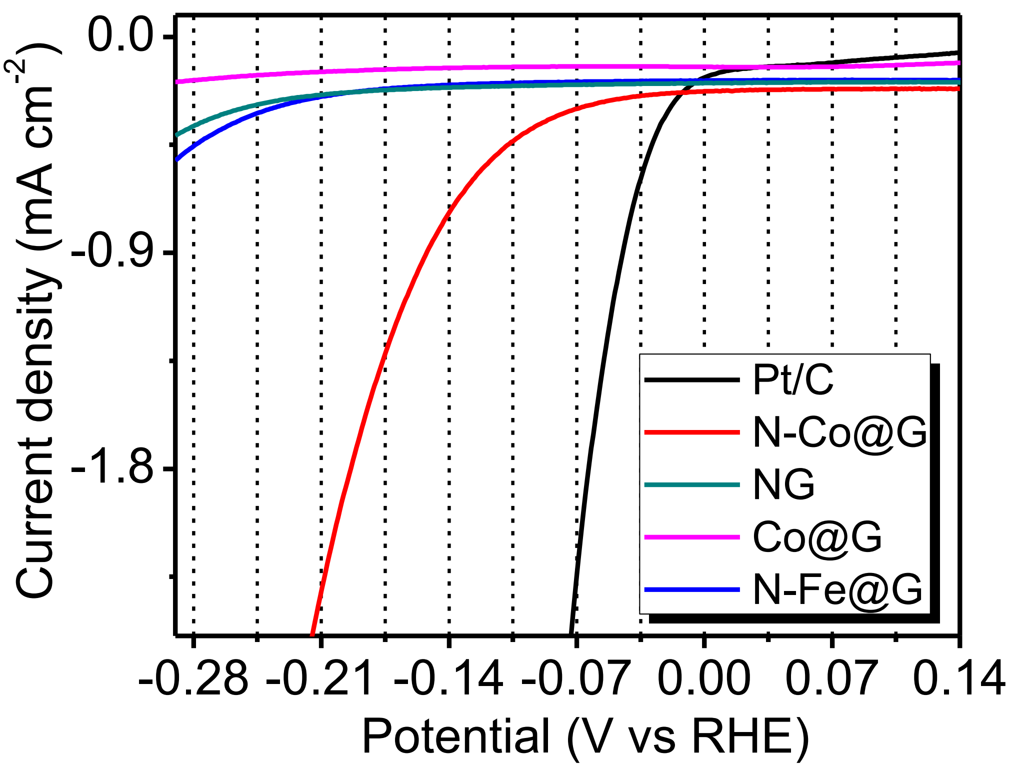

Figure S8. Polarization curves tested in alkaline solution of the corresponding samples in Figure 4d near the onset overpotential region.

Table S1. Comparisons of the HER electrocatalytic activities of N-Co@G under acidic conditions with some representative HER catalysts recently reported.

Catalyst Loading	Electrolyte	Scan rate	Onset overpotential	Overpotential to deliver 10 mA cm^{-2}	Reference
N-Co@G 285 μg cm^{-2}	0.5M H_2SO_4	5 mV s^{-1}	70 mV	265 mV	This work
Co-NRCNTs 280 μg cm^{-2}	0.5M H_2SO_4	50 mV s^{-1}	50 mV	260 mV	1
FeCo@NCNTs-NH 320 μg cm^{-2}	0.1M H_2SO_4	2 mV s^{-1}	70 mV	290 mV	2
MoP nanoparticles 360 μg cm^{-2}	0.5M H_2SO_4	2 mV s^{-1}	40 mV	125 mV	3
WS_2 nanoflakes 350 μg cm^{-2}	0.5M H_2SO_4	10 mV s^{-1}	100 mV	170 mV	4
MoS_2/RGO 285 μg cm^{-2}	0.5M H_2SO_4	2 mV s^{-1}	100 mV	150 mV	5
Defect-rich MoS_2 285 μg cm^{-2}	0.5M H_2SO_4	5 mV s^{-1}	120 mV	190 mV	6
MoB 2500 μg cm^{-2}	1M H_2SO_4	1 mV s^{-1}	100 mV	215 mV	7
Mo_2C 1400 μg cm^{-2}	1M H_2SO_4	1 mV s^{-1}	100 mV	215 mV	7
C_3N_4@NG 100 μg cm^{-2}	0.5M H_2SO_4	5 mV s^{-1}	NA	240 mV	8

Table S2. Comparisons of the HER electrocatalytic activities of N-Co@G under alkaline conditions with some representative HER catalysts recently reported.

Catalyst	Loading	Electrolyte	Scan rate	Onset overpotential	Overpotential to deliver 10 mA cm^{-2}	Reference
N-Co@G	285 μg cm^{-2}	0.1M NaOH	5 mV s^{-1}	70 mV	337 mV	This work
Co-NRCNTs	280 μg cm^{-2}	1M KOH	50 mV s^{-1}	50-100 mV	370 mV	*1*
MoB	2500 μg cm^{-2}	1M KOH	1 mV s^{-1}	100 mV	225 mV	*7*
Mo_2C	800 μg cm^{-2}	1M KOH	1 mV s^{-1}	100 mV	190 mV	*7*
$Co_{0.6}Mo_{1.4}N_2$	240 μg cm^{-2}	0.1M KOH	5 mV s^{-1}	NA	300 mV	9
C_3N_4 on FTO	NA	0.1M KOH	25 mV s^{-1}	100 mV	NA	10

References

1. Zou, X.; Huang, X.; Goswami, A.; Silva, R.; Sathe, B. R.; Mikmeková, E.; Asefa, T. *Angew. Chem. Int. Ed.* **2014**, *53*, 4372-4376.
2. Deng, J.; Ren, P.; Deng, D.; Yu, L.; Yang, F.; Bao, X. *Energy Environ. Sci.* **2014**, *7*, 1919-1923.
3. Xing, Z.; Liu Q.; Asiri, A. M.; Sun, X. *Adv. Mater.* **2014**, *26*, 5702-5707.
4. Cheng, L.; Huang, W.; Gong, Q.; Liu, C.; Liu, Z.; Li, Y.; Dai, H. *Angew. Chem. Int. Ed.* **2014**, *53*, 7860-7863.
5. Li, Y.; Wang, H.; Xie, L.; Liang, Y.; Hong, G.; Dai, H. *J. Am. Chem. Soc.* **2011**, *133*, 7296-7299.
6. Xie, J.; Zhang, H.; Wang, R.; Sun, X.; Zhou, M.; Zhou, J.; Lou, X.; Xie, Y. *Adv. Mater.* **2013**, *25*, 5807-5813.
7. Vrubel, H.; Hu, X. *Angew. Chem. Int. Ed.* **2012**, *51*, 12703-12706.

8. Zheng, Y.; Jiao, Y.; Zhu, Y.; Li, L. H.; Han, Y.; Chen, Y.; Du, A.; Jaroniec, M.; Qiao, S. Z. *Nat. Commun.* **2014**, *5*, 3783

9. Cao, B.; Veith, G. M.; Neuefeind, J. C.; Adzic, R. R.; Khalifah, P. G. *J. Am. Chem. Soc.* **2013**, *135*, 19186-19192.

10. Shalom, M.; Gimenez, S.; Schipper, F.; Cardona, I. H.; Bisquert, J.; Antonietti, M. *Angew. Chem.* **2014**, *126*, 3728-3732.